FREQUENCY STABILITY OF WAFER-SCALE FILM ENCAPSULATED SILICON BASED MEMS RESONATORS

Bongsang Kim, Rob N. Candler, Matthew Hopcroft, Manu Agarwal, Woo-Tae Park, and Thomas W. Kenny
Stanford University, Departments of Mechanical and Electrical Engineering
Address: Terman 551, Stanford, CA, 94305, USA
Tel: 650-736-0044, Fax: 650-723-3521, e-mail: bongsang@micromachine.stanford.edu

ABSTRACT

The stability of resonant frequency for single wafer, thin film encapsulated silicon MEMS resonators was investigated for both long term operation and temperature cycling. The resonant frequencies of encapsulated resonators were periocidcally measured at 25°C ± 0.1°C for > 9,000 hours, and the resonant frequency variation remained within the measurement uncertainty of 3.1 ppm and 3.8 ppm. Also, the resonantors were temperature cycled for 680 cycles between -50°C and 80°C, measuring the resonant frequency each time the temperature reached 30°C. Again, the change in resonant frequency was seen to remain within the measurement uncertainty. This demonstrates stability of resonant frequency for both long-term operation of more than a year and huge number of temperature cycling, emphasizing the stability of both the resonator and the package.

Keywords: MEMS resonator, long-term stability, resonant frequency stability, encapsulation

INTRODUCTION

Silicon based MEMS resonators are a promising technology for the replacement of quartz resonators, which are currently the dominant technology for many frequency reference applications [1], due to the potential for reduced size, cost, and power consumption, as well as integration with circuitry on the same wafer. Also, integration of the resonator structure with the IC chip can reduce parasitic losses from higher level packaging, This integration will also lead to reduced higher level packaging, which is significant when considering that packaging dominates the cost of many devices.

While there have been many breakthroughs in the field of MEMS resonators [2-5], the problem of how to package theses resonators has not yet been solved. Stability of resonant frequency over time is absolutely essential for use as a frequency reference, and the frequency stability depends on the quality of the package environment. Early work investigated the long-term stability of MEMS resonators, but the measured stability was insufficient to be used for many applications [6]. Recent work has investigated possible fatigue in thin film silicon for both single crystal and polysilicon [7, 8]. Although fatigue of thin-film silicon is not fully understood and controversial [9-12], if MEMS resonators are operated in a vacuum condition isolated from outside atmosphere and minized exposure to oxigen or humidity, the fact that silicon MEMS resonators' resonant frequency may show better performance in terms of stability has been induced [9, 13].

We have developed a wafer-scale encapsulation process for MEMS resonators and inertial sensors. Our wafer-scale encapsulation has several possible benefits, including high yield of devices on completed wafers, reduced package size (and therefore cost) due to the lack of a bonds ring, and robustness against standard post processing techniques, such as wire bonding, die handling, and injection molding of plastic [14-16]. In addition, we showed that our encapsulation process provides an effective seal against air leakage, such that it may provide excellent vacuum condition for MEMS resonators to achieve and maintain high quality factor for long-term operation [17]. We believe that the stability of the package environment also leads to stability of resonant frequency. This paper reports the first measured results for resonant frequency stability of silicon MEMS resonators fabricated within wafer-scale thin film encapsulation process.

FABRICATION

The resonators investigated here were fabricated using a single-wafer polysilicon thin film encapsulation process [17, 18]. This process involves covering unreleased MEMS devices with a sacrificial oxide layer and a 2 μm-thick epitaxial polysilicon encapsulation. The devices are released by etching this sacrificial oxide layer with a vapor-phase HF etch process through vent holes etched on the 2 μm thick silicon layer. The encapsulation is then resealed by a ~25 μm-thick epitaxial polysilicon deposition and planarized via chemical-mechanical polishing (CMP). The 25 μm-thick encapsulation is etched to provide isolation for the electrical contacts, which are routed *through* the highly conductive polysilicon encapsulatoin. Finally, oxide and metal layers are deposited to provide electrical contact and insulation to the resonator. Figure 1 shows a schemetic of our encapsulation process and Figure 2 shows an SEM cross section view of the resonator used for the stability test.

The encapsulation creates a hermitic seal for the resonators and insulates them against outside conditions such as particles, humidity, gases, etc. The quality of this encapsulation was investigated in our previous work [17].

The two resonator designs used in this work are actuated and sensed by electrostatic force (Fig. 3). Both of them are specifically designed with a single mechanical support in the middle of the structure to minimize the possibilities of induced stress from thermal expansion of different materials or residual stress of abjecnt layers. The electrostatic driving force is applied at the "Stimulus" electrodes and the resonator output is sensed through the "Response" electrodes, with a DC bias applied to the resonator structure. Temperature coefficient of resonant frequency(TCf), resonant frequency sensitivity to the environmental temperature change is experimentally acquried as -27ppm/°C for design A resonators and -33ppm/°C for design B resonators respectively at room temperature. These values depend on temperature coefficient of Young's modulus of silicon and resonator geometry. Temperature in the chamber was maintained within ±0.1°C range which corresponds to ±2.7ppm for design A resonators and ±3.3ppm design B resonators respectively based on their TCf values. In addition, due to the measurement setup, the measurement has additional error range of ±0.4ppm. Based on this information, total error range is ±3.1ppm and ±3.7ppm for design A resonators and design B resonators respectively. The main characteristics of design A resonators and design B resonators are summarized in table 1.

LONG-TERM STABILITY AT CONSTANT TEMPERATURE

Measurement setup diagram is shown in figure 4. Long-term frequency drift of these MEMS resonators was examined by monitoring 6 separate resonators. Each resonator was excited and measured approximately every 30 minutes for more than one year (about 10,000 hours) using an Agilent 4395A network analyzer. To minimize temperature-related frequency variations, the resonators were installed in a temperature-controlled chamber which provides test temperature within ±0.1°C error range.

Figure 5 represents monitored resonant frequency of MEMS resonators. The discontinuities in the data represent periods when the test was stopped for maintenance or improvement. As shown in the figure, the resonant frequency of none of the six resonators measured, has drafted more than its measurement error range. A little instablity of resonant frequency during first 500 hours of operation (~3ppm) can be seen. However, the instability, which is < 5ppm, is not unreasonable, as typical quartz crystal resonators exhibit up to 10 ppm of burn-in drift during the first few days to weeks of operation [19]. Also, one clue exists that suggests that the initial instability is a problem with the initial measurement setup and not burn in; the two resonators which were started at 3,000 hours (and had never been previously resonated) did not show any initial instability, which suggests that there is not a material change causing a shift in resonant frequency.

To show more detail, a zoomed in plot of the first resonator is shown in figure 6. In this figure, we can see resonant frequency for both of resonators are remained in error ranges,±3.1ppm and ±3.7ppm for design A resonators and design B resonators respectively as explained before. This was true for all the resonators monitored in this experiement.

STABILITY DURING AND AFTER TEMPERATURE CYCLE

Another experiment was performed to examine resonant frequency stability after rapid environmental temperature changes. If there is axial stress on the resonator beam due to thermal expansion, it can cause change in resonant frequencies of MEMS resonators [20] or cracking in the encapsulation. Again, the MEMS resonators used in these experiments are single anchored, thus they are expected to be immune to axial stress derived from differential expansion of layers in the encapsulated silicon die.

Resonant frequency of two installed design A resonators was measured in between each temperature cycle for almost 700 cycles from –50°C to +80°C (Fig.7 (a)). The temperature inside the chamber ramped up to 80°C and down back to 30°C. After that it was held for 30 minutes to reach thermal equilibrium in the temperature chamber. Then the resonant frequencies of all the MEMS resonators were measured. The temperature was then ramped down to –50°C and back to 30°C to measure the resonant frequencies again.

To date, almost 700 temperature cycles have been performed, and all the measurements were performed at 30±0.1°C. Again drift in resonant frequency was maintained in measurement error range (Fig.7 (b)). In addition resonant frequency difference between measurement after high temperature cycles and after low temperature cycles stayed within the measurement error. The observed frequency shift is most likely related to slight temperature gradients within the apparatus at the time of the measurements.

HYSTERESIS OF RESONANT FREQUENCY

The next experiment performed to measure resonant frequency every 10°C while the temperature was ramping up and down between –10°C and +80°C. Again design A resonator was used in this experiment. The temperature in the chamber was increased in steps of 10°C, and at each step, the chamber was held for 30 minutes and allowed to reach thermal equilibrium before the resonant frequency was measured. The same process was repeated for decreasing temperature from +80°C to –10°C As shown in Fig. 8, no trend between temperature increasing and decreasing cases has been found and the difference in resonant frequency was remained again in measurement error range.

The result from these separate experiments indicate that there is no significant residual stress or differential thermal expansion which might affect resonant frequency stability for rapid changes in environmental temperature.

CONCLUSIONS

For the first time, resonant frequency stability of wafer-scale encapsulated MEMS resonators has been investigated in various ways. We have shown that the long-term aging rate of these resonators is equivalent to commercial quartz crystal

resonators. Also, unlike quartz resonators, no initial aging or stabilization period was found. In addition no measurable hysteresis was found.

This improved performance is attributed to the clean, high-temperature fabrication process used to encapsulate these resonators, which suggests that the drift and hysteresis problems observed in other MEMS resonators have never been fundamental, but rather have always been due to their operating environment. Our encapsulation process is able to provide an effective shield for resonant frequency stability for MEMS resonators.

Currently, resonant frequency stability of these resonators with self-oscillating circuits is being examined. With the help of self-oscillating circuits, these resonators will operate continuously at their resonant frequencies. Also, resonant frequency stability related to material fatigue or aging will be investigated in the near future. We plan to build a test set-up which will provide a more stable operating temperature further refine stability measurement of MEMS resonators. We expect that these improvements will allow us to show more accurate and precise results about resonant frequency stability for MEMS resonators in the near future.

ACKNOWLEDGEMENTS

This work was supported by DARPA HERMIT (ONR N66001-03-1-8942), Bosch Palo Alto Research and Technology Center, a CIS Seed Grant, The National Nanofabrication Users Network facilities funded by the National Science Foundation under award ECS-9731294, and The National Science Foundation Instrumentation for Materials Research Program (DMR 9504099). The authors would especially like to thank Gary Yama[1], Markus Lutz[2], and Aaron Partridge[2] for their guidance and assistance, without whom this work would not have been possible ([1]Robert Bosch Corporation, [2]Robert Bosch Corporation, currently at SiTime). We would also like to thank John R. Vig from the U.S. Army Communications Electronics Command for his valuable advice.

REFERENCES

1 J. Vig and A. Ballato, *Ultrasonic Instruments and Devices,* Academic Press, Inc., 1999, Ch.7 Freqeuncy Control Devices, pp. 637-701.

2 Z. Hao, et al., VHF Single Crystal Silicon Elliptic Bulk-Mode Capacitive Disk Resonators; Part I: Design and Modeling, *IEEE Journal of Microelectromechanical Systems*, Vol. 13 (2004) 1054-1062.

3 S. Pourkamali, et al., VHF Single Crystal Silicon Elliptic Bulk-Mode Capacitive Disk Resona, *IEEE Journal of Microelectromechanical Systems*, Vol. 13 (2004) 1054-1062.

4 C. Nguyen, *High-Q micromechanical oscillators and filters for communications, IEEE International Symposium on Circuits and Systems. Circuits and Systems in the Information Age ISCAS '97, Hong Kong, 9-12 June 1997, pp. 2825-2828.*

5 C. Nguyen and R. Howe, Integrated CMOS micromechanical resonator high-Q oscillator, *IEEE Journal of Solid-State Circuits*, Vol. 34 (April 1999) 440-455.

6 H. Guckel, et al., *Polysilicon resonant microbeam technology for high performance sensor applications, Proceedings of the 5th IEEE Solid-State Sensor and Actuator Workshop, Hilton Head Island, SC, USA, Jun 22-25 1992, pp. p.153-156.*

7 C. Muhlstein, et al., High-cycle fatigue of single-crystal silicon thin films, *Journal of Microelectromechanical Systems*, Vol. 10 (2001) 594-600.

8 C. L. Muhlstein and R. O. Ritchie, High-cycle fatigue of micron-scale polycrystalline silicon films: fracture mechanics analyses of the role of the silica/silicon interface, *International Journal of Fracture*, Vol. 119-120 (2003) 449-474.

9 C. Muhlstein, et al., Fatigue of polycrystalline silicon for microelectromechanical system applications: Crack growth and stability under resonant loading conditions, *Mechanics of Materials*, Vol. 36 (2004) 13-33.

10 H. Kahn, et al., Dynamic fatigue of silicon, *Current Opinion in Solid State & Materials Science*, Vol. 8 (2004) 71-76.

11 H. B. Kahn, R; Bellante, JJ; Heuer, AH, Fatigue failure in polysilicon not due to simple stress corrosion cracking, *Science*, Vol. 298 (2002) 1215-1218.

12 P. Shrotriya, et al., Fatigue Damage Evolution in Silicon Films for Micromechanical Applications, *Experimental Mechanics*, Vol. 43 (2003) 289-302.

13 M. Koskenvuori, et al., Long-term stability of single-crystal silicon microresonators, *Sensors and Actuators, A: Physical*, Vol. 115 (2004) 23-27.

14 W.-T. Park, et al., *Wafer Scale Encapsulation of MEMS Devices, INTERPACK'03 The Pacific RIM/ASME International Electronic Packaging Technical Conference and Exhibition, Maui, Hawaii, USA, July 6-11, 2003,*

15 W.-T. Park, et al., *Wafer Scale Film Encapsulation of Micromachined Accelerometers, 12th International Conference on Solid-State Sensors, Actuators, and Microsystems (Transducers 2003), Boston, MA, USA, June 8-12, 2003, pp. 1903-1906.*

16 R. Candler, et al., *Single Wafer Encapsulation of MEMS Devices, IEEE Transactions on Advanced Packaging, Aug. 2003, pp. 227-232.*

17 B. Kim, et al., *Investigation of MEMS resonator characteristics during long-term and wide temperature operation, 2004 ASME International Mechanical Engineering Congress and RD&D Expo, Anaheim, California USA, November 13-19, 2004,*

18 A. Partridge, et al., *New thin film epitaxial polysilicon encapsulation for piezoresistive accelerometers, MEMS 2001. 14th IEEE International Conference on Micro Electro Mechanical Systems, 21-25 Jan. 2001, pp. 54-59.*

19 J. R. Vig and T. R. Meeker, *The aging of bulk acoustic wave resonators, filters and oscillators, the 45th Annual Symposium on Frequency Control 1991, Los Angeles, CA, USA, May 29-31 1991, pp. 77-101.*

20 J. A. Kusters and J. R. Vig, Hysteresis in quartz resonators-- A review, *IEEE Transactions on Ultrasonics, Ferroelectrics and Frequency Control*, Vol. 38 (1991) 281-290.

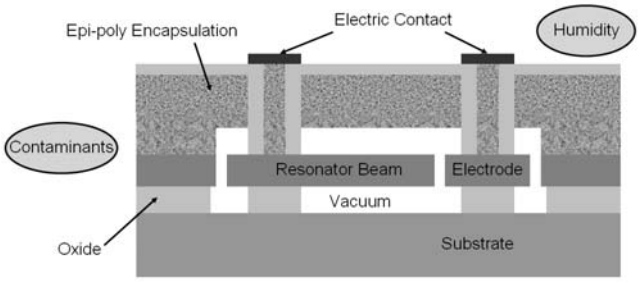

Figure 1. Basic schematic for epi-seal encapsulation process. Resonator is released by HF vapor etching of sacrificial oxide, and epi-poly silicon is deposited to seal the cavity. (Not to scale)

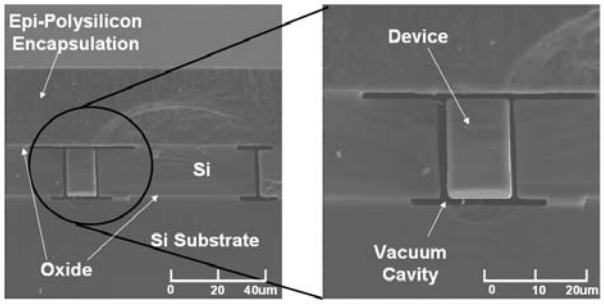

Figure 2. SEM picture of cross-section view of the device fabricated by epi-seal encapsulation process. The polysilicon cap layer creates a hermitically sealed enclosure. The pressure in the cavity is determined to be less than 1.5 Pa

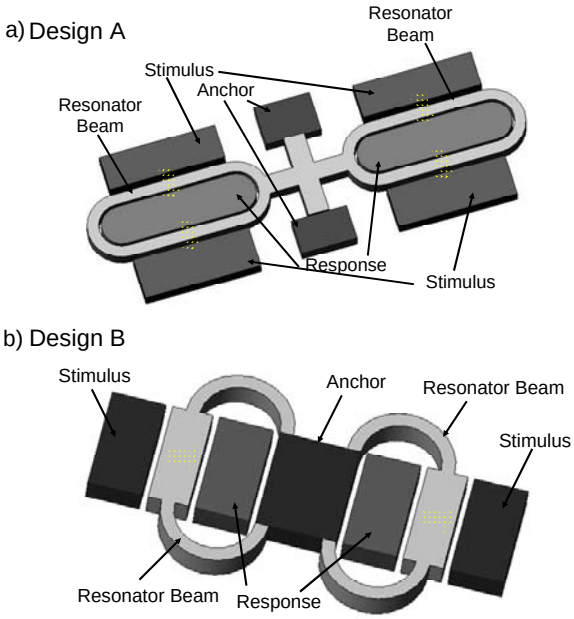

Figure 3. Perspective view schematic of the MEMS resonator designs used in the experiment. Driving force is applied at the "Stimulus" electrodes and the resonator output is sensed through the "Response" electrodes. The resonator beams are moved by electro static force.

Resonator Design	Design A	Design B
Resonant Freq.	~155kHz	~129kHz
Quality Factor	~30,000	~50,000
TCF	~27ppm/°C	~33ppm/°C
Measurement Uncertainty	~3.1ppm	~3.7ppm

Table 1. Main characteristics of MEMS resonators used for the resonant frequency stability test

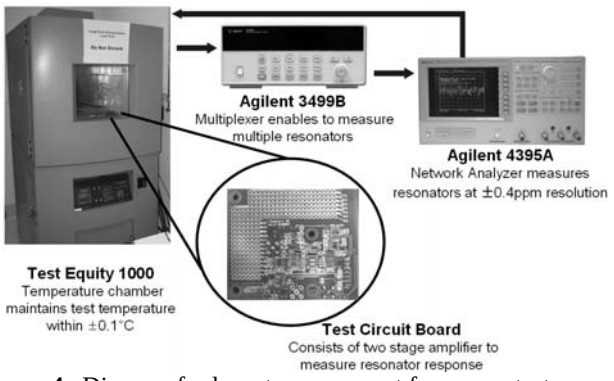

Figure 4. Diagram for long-term resonant frequency test. Circuit boards with embedded resonators are installed in a temperature chamber which maintains the test temperature in ±0.1°C range. A network analyzer measures resonant frequency of each resonator through a multi-plexer which enables to measure multiple resonators one by one. The measurement resolution of resonant frequency is approximately ±0.4ppm.

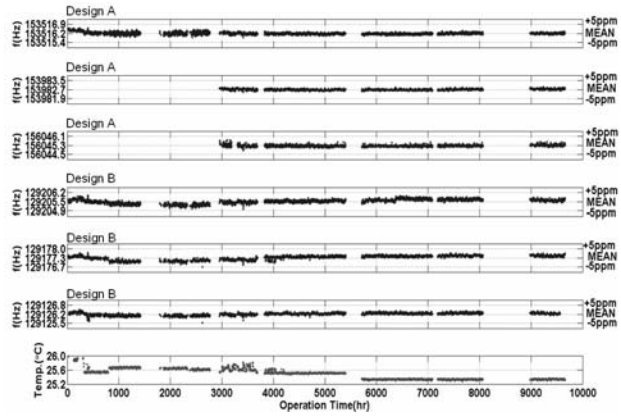

Figure 5. Plot of resonant frequency vs time for the resonators used in the long-term aging test. The top three are design A resonators and the next three are design B resonators. The temperature of the oven containing the resonators is given at the bottom. During 10,000 hrs operation, no trend of resonant frequency shift could be detected. Drift in resonant frequency is only within measurement error range, which is limited by instability of experimental temperature and resolution of network analyzer setup.

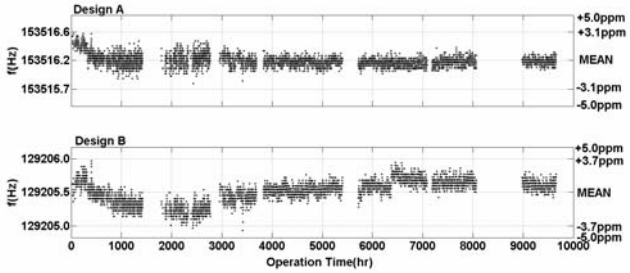

Figure 6. Plot of resonant frequency vs time for one of design A resonators and design B resonators. Except for a few outliers resonant frequency drift are maintained within less than ±3.1ppm and ±3.7ppm respectively, which are possible maximum measurement error of design A resonators and design B resonators.

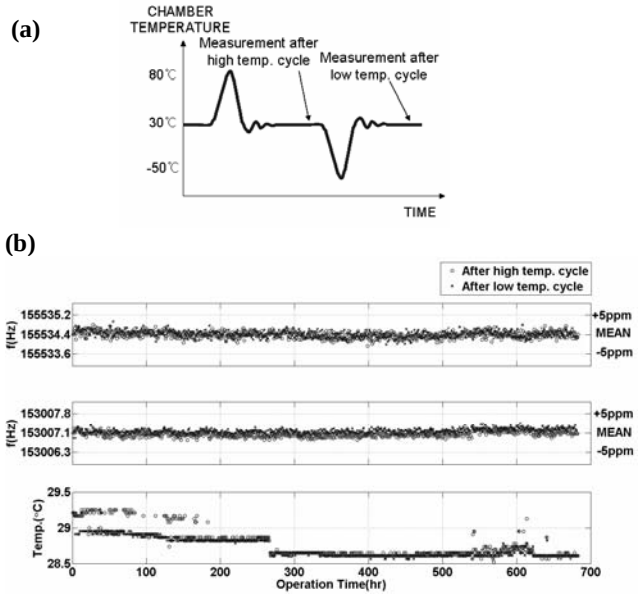

Figure 7
(a) Resonant frequency of the MEMS resonators was measured at 30°C after the temperature inside the chamber was cycled between –50°C and 80°C. Every measurement took place after holding for about 30 minutes to reach thermal equilibrium.
(b) Plot of resonant frequency vs temperature for temperature cycling test. Resonant frequencies are measured at 30°C after high temperature cycle (O) and after low temperature cycle (X). This result suggests long-term stability of resonant frequency even after large number of wide temperature cycle.

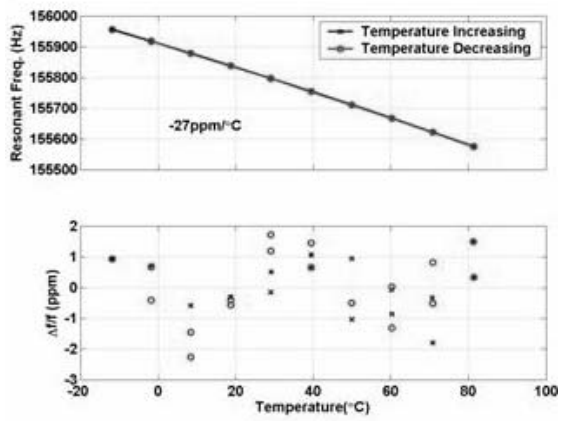

Figure 8 The upper plot shows resonant frequency vs temperature for hysteresis test. The lower plot demonstrates the error of resonant frequencies with respect to the interpolated resonant frequencies at that temperature. Again, measurements following high temperature cycle are represented by “O” and measurements following low temperature cycle are represented by “X”. So far no trend between temperature increasing and decreasing cases has been found. While cycling the environmental temperature, resonant frequencies are measured every 10°C.